

CFD ANALYSIS OF HIGH SWIRLING FLOW IN GAS CYCLONES

İsmail Ozan Sert¹ and Sitk Uslu²
TOBB University of Economics and Technology,
Ankara, Turkey

Onur Bař³
TED University
Ankara, Turkey

ABSTRACT

The numerical study of the high swirling flow in the gas cyclone is conducted by performing CFD analysis. Modeling the turbulence characteristics of the high swirling flow is a challenging phenomenon considering anisotropic structure of the Reynolds stress tensors. Hence the numerical results of different turbulence models are calculated for two different gas cyclone types. The performance of the turbulence models are compared with the available experimental data in the literature by evaluating the axial and tangential mean velocity components. Unlike most Industrial CFD applications, it is observed that the RANS turbulence models are not capable of capturing flow characteristics of the high swirling flows. The numerical estimations of the RSM and DDES models are found more realistic and reasonable with respect to $k-\omega$ SST RANS model.

¹ PhD Candidate, Email: isert@tai.com.tr

² Dr. in a Mechanical Engineering Department, Email: suslu@etu.edu.tr

³ Dr. in a Mechanical Engineering Department, Email: onur.bas@tedu.edu.tr

INTRODUCTION

In today's world, gas cyclones are one of the most used filtration systems due to their high separation efficiency for a wide range of type and size of the flow impurities. The cyclones are employed from petro-chemical applications to our daily use cleaning devices with their compactness and simplicity. The cyclone technology has been used and investigated since the 20th century, the fair prediction of the high swirling flow passing through the cyclone tube is still important to maximize the efficiency.

Initially, the semi-empirical or theoretical prediction methodologies [Barth 1956, Leith and Licht, 1972, Iozia and Leith, 1989] are implemented to evaluate the basic design parameters pressure drop and the separation efficiency. With improving technologies, the computational fluid dynamics software adoption rapidly increased as with most other numerical calculation processes. Hence the design process of the gas cyclones have been mostly assessed with CFD applications [Griffiths, 1996, Gimbutu 2005]. Another challenging issue to predict the high swirling flow in the gas cyclones is to determine turbulence characteristics. Slyvia et al. [Slyvia, 2011] performed a numerical study of the turbulence model performances by a comparison of the experimental data of Wang et al. [Wang 2005]. Since the high swirling flow turbulence stresses are anisotropic, first order closure models such as Reynolds Averaged Navier-Stokes (RANS) struggle to predict flow characteristics. Slyvia et al. concluded that only RSM turbulence model was capable of reliable flow field predictions compared to the RANS models. Hoekstra et al. [Hoekstra, 1999 and 2000] performed comprehensive numerical and experimental gas cyclone studies to outline the complex nature of the swirling flow in gas cyclones. The swirl tube and Stairmand cyclones were numerically and experimentally investigated, the axial and tangential velocity components were calculated and compared. It is observed that the flow field which has been represented by RSM turbulence model was in better agreement with the experimental data.

In this study, the experimental findings of Hoekstra et al. [Hoekstra 1999 and 2000] is numerically investigated with various turbulence models to understand the high swirling flow characteristics. The behavior of the high swirling flow will be modelled by RANS, RSM and DES turbulence models and their prediction performances will be evaluated.

METHOD

The numerical analysis of high swirling flow in gas cyclones are performed using Starccm+ commercial CFD solver, which is a 3D Navier-Stokes solver with cell-centered 2nd order spatial discretization. As described in the experimental studies of Hoekstra et al. [Hoekstra 1999, 2000], two different gas cyclone type, Stairmand and Swirl tube geometries are modeled. The geometry, grid and solver methodology are explained in the following sub chapters.

Geometry and Grid Distributions

The swirl tube and the Stairmand cyclone geometric parameters that are shown in Figure 1 which are used on the experimental and numerical studies of the Hoekstra et al. [Hoekstra, 1999; Hoekstra, 2000].

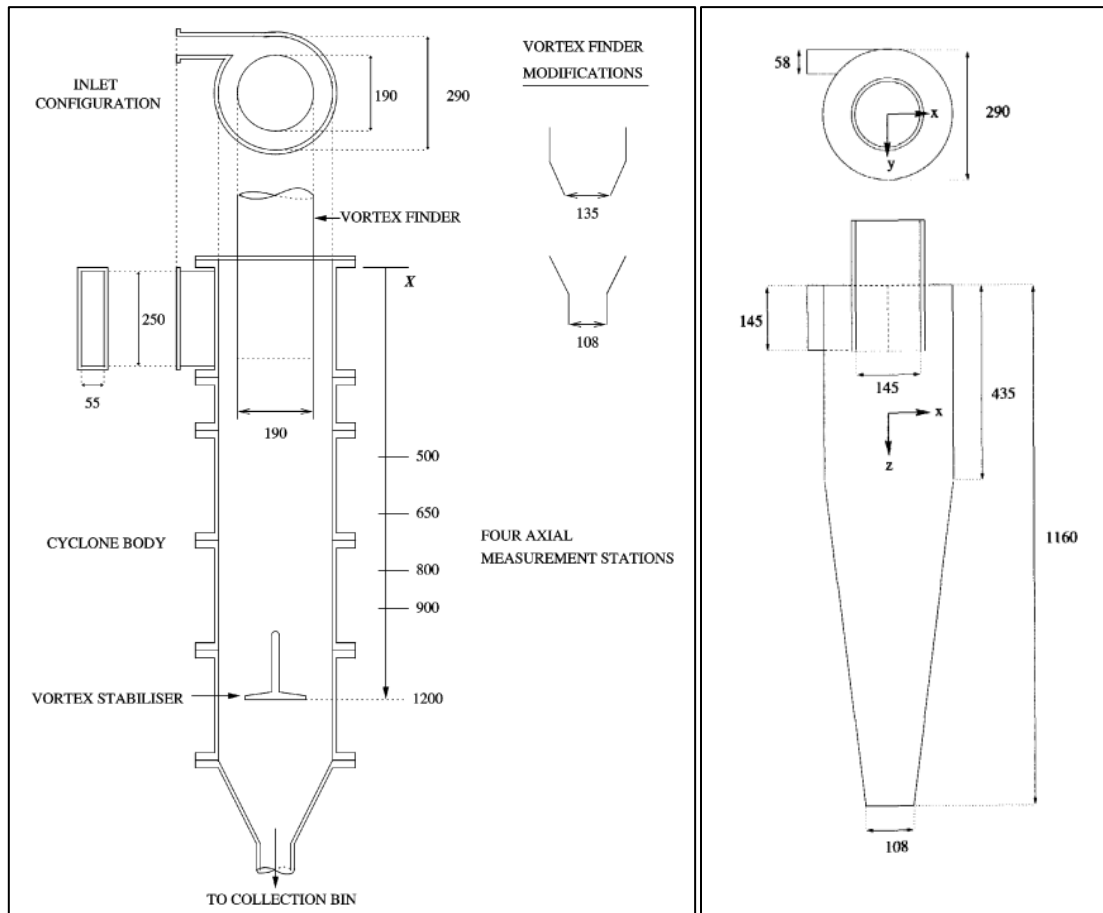


Figure 1: Swirl tube (left) and Stairmand (right) cyclone geometries [Hoekstra, 2000].

Both cyclones have 290 mm outer tube diameter with scroll type inlets. The inner tube diameters of swirl tube and Stairmand cyclone are 190 and 145 mm, respectively.

The geometries are represented by three different polyhedral surface and volume grid distributions in order to satisfy grid and solver independency. Considering the order of Reynolds numbers (10^4 - 10^5), the first layer thickness is selected as 10^{-5} m to ensure the non-dimensional first layer parameter $y^+ \sim 1$. The near wall region is defined with 30 layers to obtain sufficient boundary layer resolution. In Figure 2, three different grid distributions on the symmetry planes are shown for Stairmand cyclones.

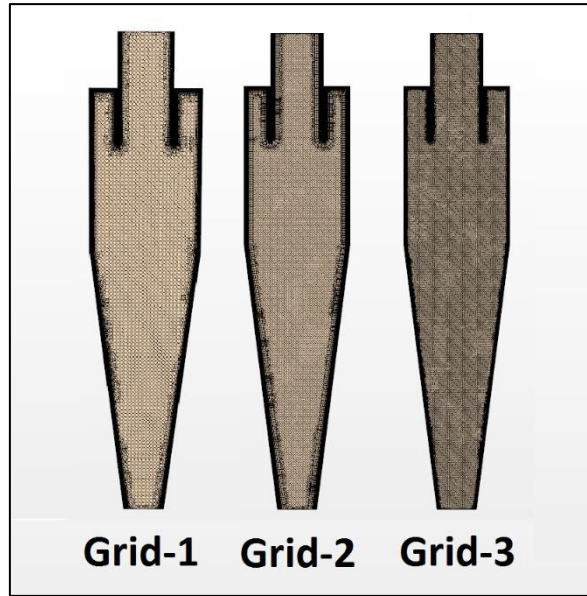


Figure 2: Stairmand cyclone symmetry plane grid distributions.

A similar grid distribution methodology is applied for the swirl tube geometry. The grid distribution properties and the related CFD calculated pressure drops between inlet and clean outlet (vortex finder outlet) surfaces are listed in Table 1. It is observed that the pressure drop values are converged with increasing grid size.

Table 1. Grid information of the blocks.

Grid Distribution #		Cell Elements #		Pressure Drop (Pa)	
Swirl Tube	Stairmand	Swirl Tube	Stairmand	Swirl Tube	Stairmand
1		1.2 M	2.0 M	92	1245
2		3.1 M	4.2 M	84	1205
3		9.1 M	9.5 M	84	1201

In order to satisfy the results with independent grid resolutions, three grid distributions are analyzed by employing RSM turbulence model with 6.2 m/s and 20 m/s uniform inlet velocity boundary conditions for the swirl tube and Stairmand cyclone geometries respectively. The grid volume elements are increased approximately by a factor of 2.5 until the main integral flow parameter (which is pressure drop in this case) is converged.

Not only the integral flow parameters, but also the distributions such as tangential and axial velocity components are compared for the grid independency studies. The velocity components of swirl tube and Stairmand cyclones are obtained at the axial stations which are $z/D=1.75$, and 0.75 , respectively as shown in Figure 3.

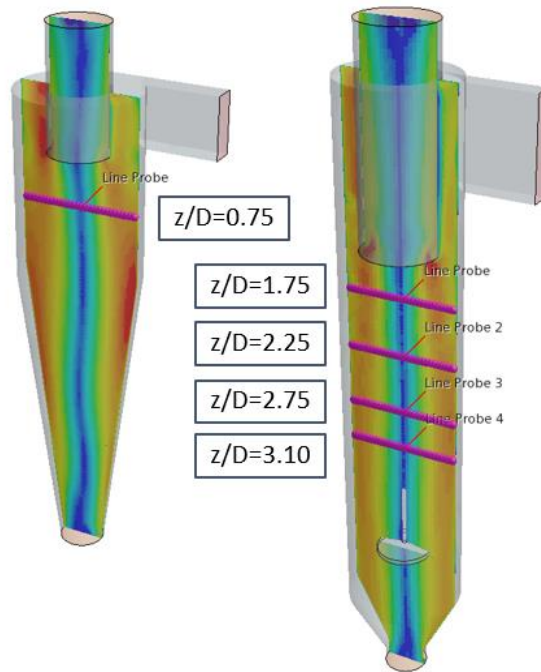


Figure 3: Stairmand (left) and Swirl tube (right) axial line configurations.

The velocity components along the line probes are compared for both cyclones with each grid distributions.

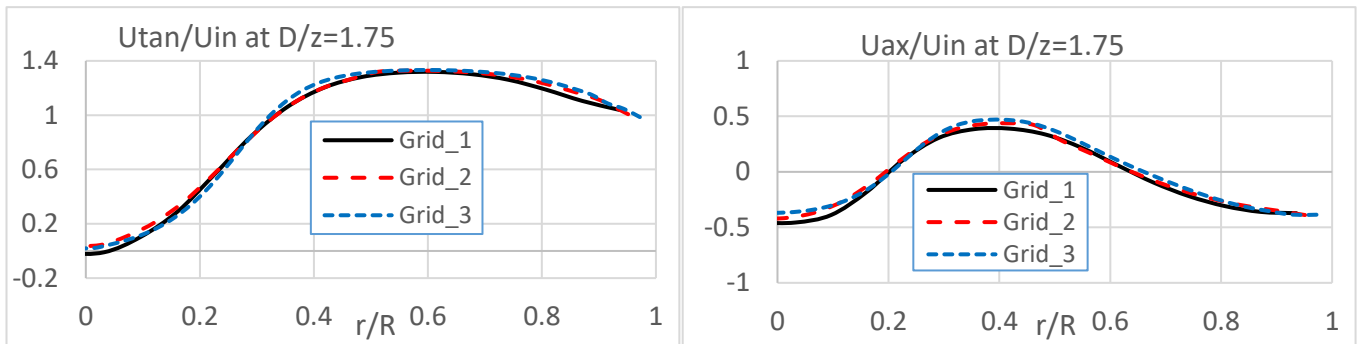


Figure 4: Swirl tube tangential (left) and axial (right) velocity distributions along the radius.

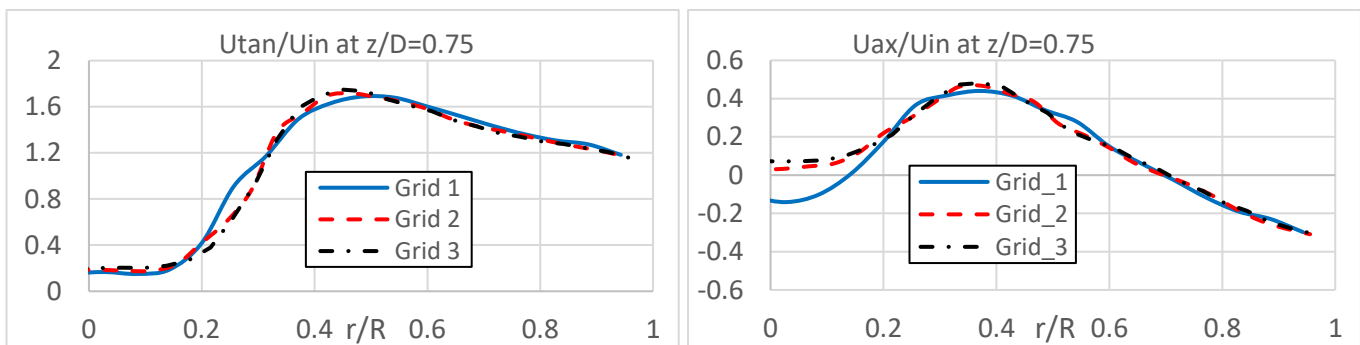


Figure 5: Stairmand tangential (left) and axial (right) velocity distributions along the radius.

In Figure 4 and 5 it is shown that the velocity distributions of the Grid 2 and 3 are very similar. The dissimilarities are investigated using L2 norm parameters, which are varied between 14 and 23 %. The maximum tangential velocity differences are obtained 11 and 13 % respectively for the swirl tube and Stairmand cyclone. On the other hand, the maximum axial velocity component differences are recorded as 8.5 and 5.2 %. The maximum differences are found at the center zone of the tubes, which have considerably low velocity magnitudes. Considering the computational time and effort, Grid distribution 2 was chosen to be employed for future CFD analyses.

Mathematical Modelling

The highly swirling flow passing through the cyclone geometries are modeled by the commercial CFD software StarCCM+. The 2nd order cell centered spatial discretization is employed with compressible coupled implicit scheme under steady state and time-dependent conditions. The unsteady analyses are conducted by 2nd order temporal discretization with 1.0 E-5 second time-step till 2 second physical time. Different turbulence models such as k- ω SST, RSM and DES are investigated to compare the prediction capabilities. The solver settings are selected as steady and/or unsteady according to turbulence model compatibilities.

Turbulence Modelling

The effect of selected turbulence models on the high swirling flows are investigated. First, the well-known 2 equation RANS k- ω SST turbulence model which is commonly used in internal flow applications is employed. The RANS models are based on the Boussinesq approach, which introduced the turbulent eddy viscosity concept to include the turbulence stresses. This approach is widely used in the industry because of prompt and fairly reasonable predictions. Since the RANS models assumes the turbulence stress isotropic, it has poor performance at dealing flows with high rotation and large strains .

Considering the challenging nature of the high swirling flow, special care is necessary to include the anisotropic behavior of the turbulence. Hence, the Reynolds Stress Model (RSM), which implements additional six partial differential equations for normal and shear Reynolds stresses, is used. The RSM model involves working with the Reynolds tensor instead of its trace.

Due to the unsteady characteristics of the swirling flow, DES (Detached eddy simulation), which is a hybrid model of RANS and LES approaches, is utilized. While its LES mode inherently handles anisotropy, the RANS mode still has isotropic assumptions due to Boussinesq approach.

RESULTS

The flow in the selected cyclones are modeled by the CFD analyses and the results are compared with the experimental data. The effects of the turbulence models on the flow characteristics are outlined. The velocity components along the tube radius are calculated at the axial measurement stations, which are described in the Figure 3.

The axial measurement station of the Stairmand is determined as $z/D=0.75$, while swirl tube measurements are collected from $z/D=1.75, 2.25, 2.75, 3.10$. The velocity components are non-dimensionalized by uniform velocities, which are introduced at the scroll inlets as 6.2 and 20 m/s respectively, swirl tube and Stairmand cyclones.

Stairmand Cyclone

The Stairmand cyclone tangential and axial velocity distributions along the tube radius are compared with the experimental data at the $z/D=0.75$ measurement station

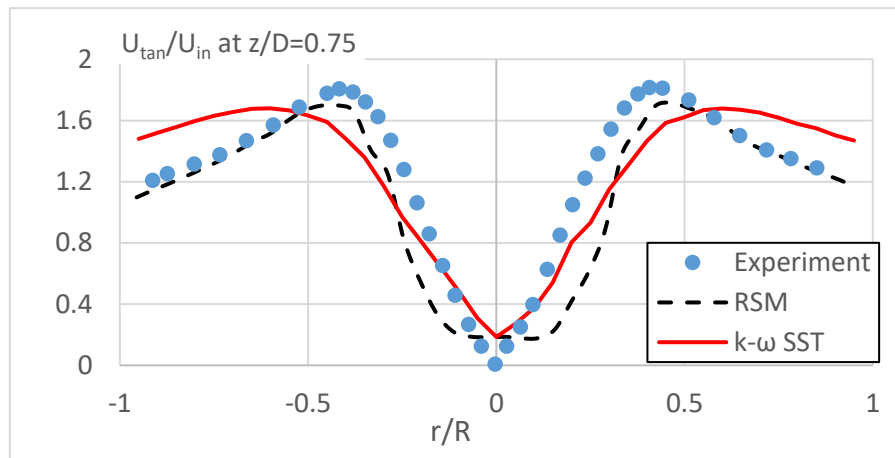


Figure 6: Stairmand cyclone tangential velocity distribution comparison.

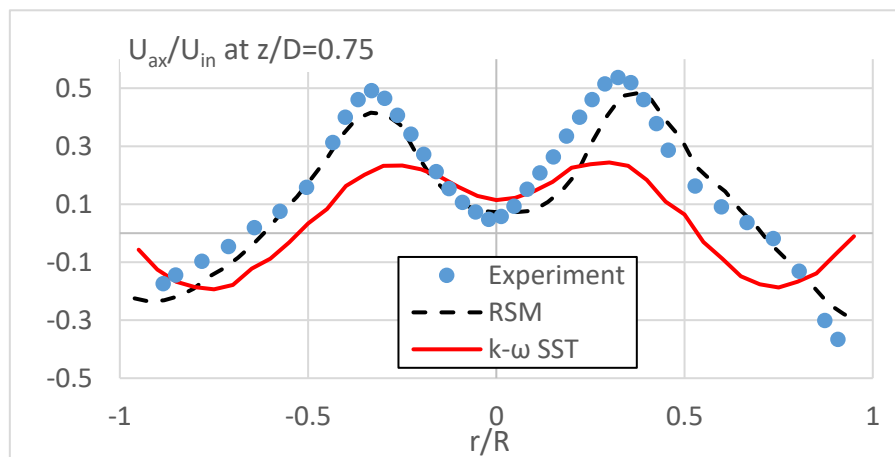


Figure 7: Stairmand cyclone axial velocity distribution comparison.

In Figure 6, the $k-\omega$ SST and RSM turbulence model tangential velocity components are compared with experimental data. While $k-\omega$ SST predictions are superior compared to the RSM model at the center of the tube, this finding changes to the contrary towards the tube walls.

In Figure 7, it is clearly observed that the $k-\omega$ SST model is unable to predict the axial velocity characteristics along the tube radius. On the other hand, RSM model simulation is able to capture the flow characteristics of the experimental data. The tangential and axial velocity component distributions on the symmetry plane obtained by $k-\omega$ SST and RSM model are compared in Figure 8. Because of the unsteady flow characteristics, mean velocity distributions are displayed for the steady-state analyses.

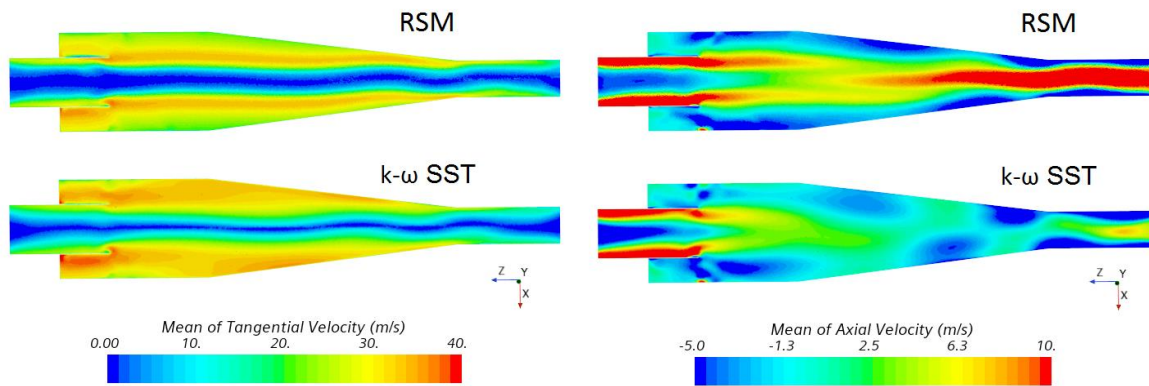


Figure 8: Mean tangential (left) and axial (right) velocity distributions on symmetry plane of the Stairmand cyclone.

In Figure 8, it is observed that the velocity components are obviously distinguishable at the center of the cyclone, which is similar with radial distributions velocity distributions shown in Figure 6 and 7. Particularly, the axial velocity components differ at the two exits, which effects the overall pressure drop.

Table 2. Stairmand Cyclone Pressure Drop Comparison.

Turbulence Model	Pressure Drop (Pa)	Discrepancy (%)
RANS k- ω SST	1627	37.8
RSM	1205	2.0
Experiment	1181	--

The pressure drop between the inlet and the clean air outlet is integrated and compared with the experimental data in Table 2.

The low fidelity velocity predictions of the k- ω SST model causes overestimated pressure drop along the cyclone as shown in the Table 2. While the discrepancy of the RSM model is found as 2.0 %, this value is increased to 37.8 % for k- ω SST model.

Swirl Tube

Similarly, the velocity components of the swirl tube cyclone are compared with the experimental data at four different measurement stations which are located $z/D=1.75, 2.25, 2.75, 3.10$. The numerical results are obtained by RANS $k-\omega$ SST, RSM and DES turbulence models.

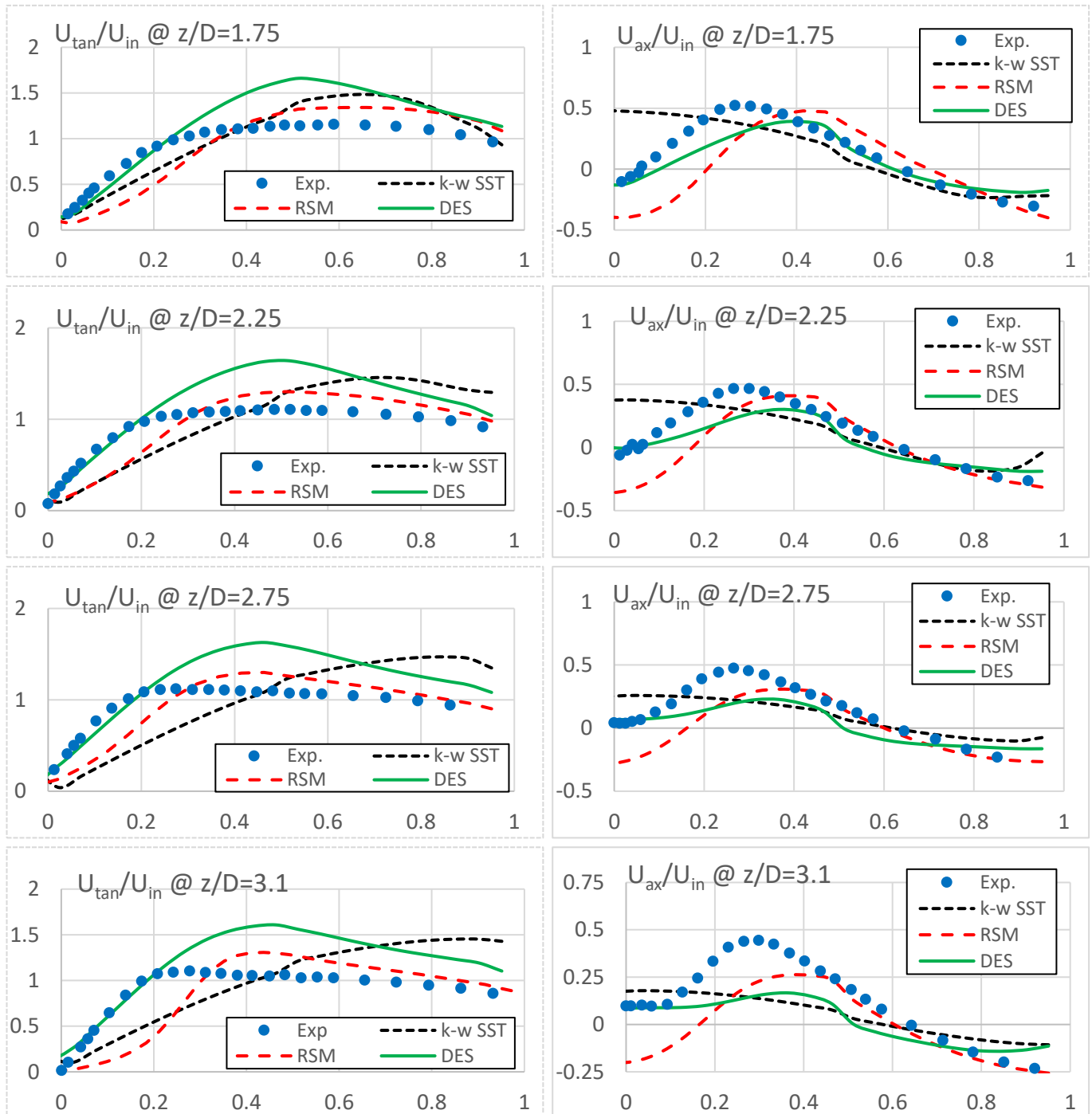


Figure 9: Swirl Tube cyclone velocity distribution comparison at located $z/D=1.75, 2.25, 2.75, 3.10$.

In Figure 9, tangential and axial velocity components at four different axial stations are compared with experimental data. Unlike the Stairmand cyclone analyses, all turbulence model predictions are slightly far from the experimental data.

Neither velocity distributions nor the magnitudes are successfully represented by the $k-\omega$ SST turbulence model. On the other hand, the RSM and DES models have fairly good predictions depending on the tube radial locations.

While the velocity characteristics are well predicted by the RSM model, the velocity magnitudes particularly at the tube center are very distinguishable in comparison to experimental data.

Unlike RSM, DES model tangential velocities are in very good match at the center zone ($r/R < 0.2$) but the predictions overshoot as the radius increases. DES axial velocity components are very well predicted for most of the region. However, the axial velocity amplitudes are underestimated and diffused as axial locations.

The tangential and axial velocity component distributions on the symmetry plane is compared in Figure 10 and 11. The $k-\omega$ SST and RSM analyses are performed under steady-state conditions while unsteady settings are employed for the DES simulation. Similar with Stairmand cyclone analyses, the mean velocity values are presented to avoid fluctuations. The unsteady analysis is performed for 2 seconds physical time with 1×10^{-5} time step and 10 inner iterations. The 2-second time averaged distributions are displayed in Figure 10 and 11.

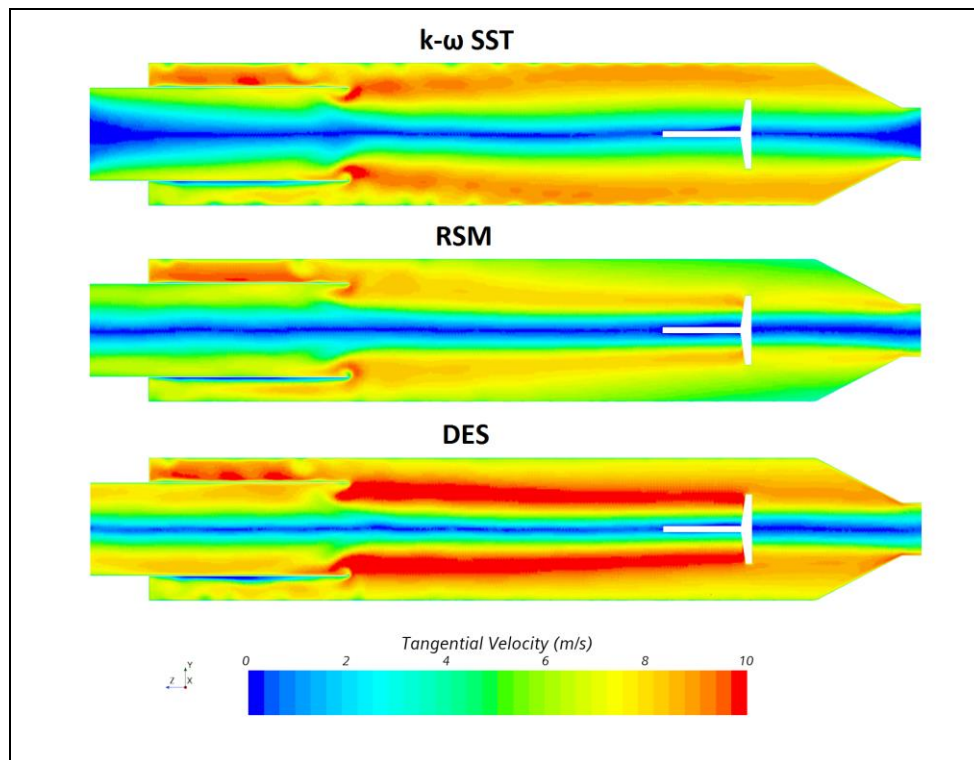


Figure 10: Mean tangential velocity distributions on symmetry plane of the Swirl Tube.

The tangential velocity components differ for each turbulence model. However, the DES components are distinguishably higher than the others.

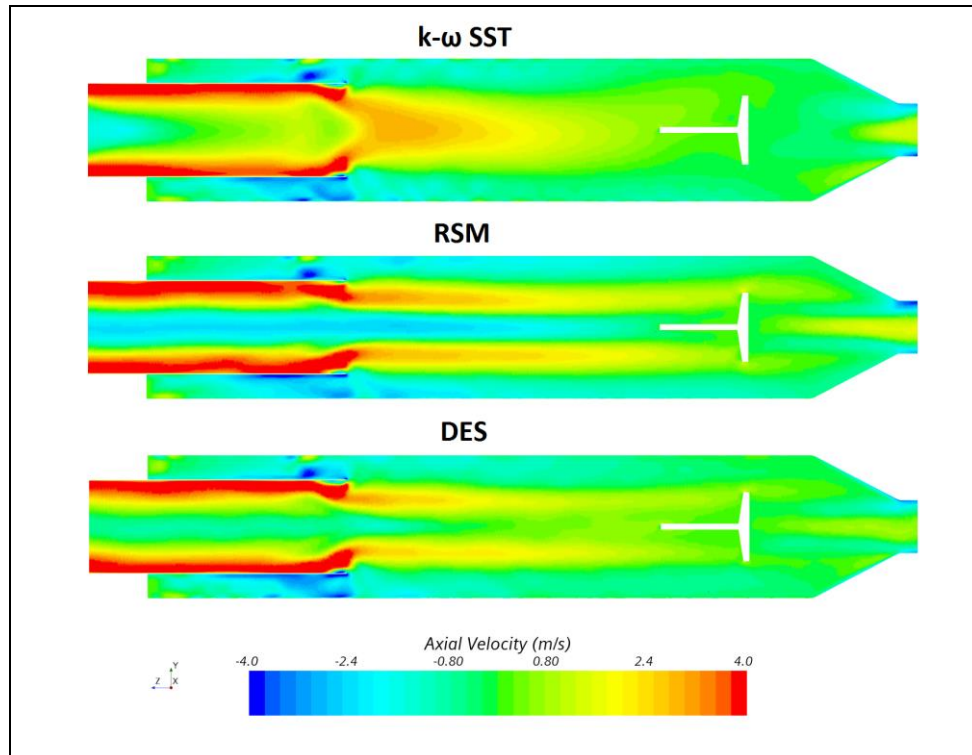


Figure 11: Mean axial velocity distributions on symmetry plane of the Swirl Tube.

In Figure 11, center of the vortex finder (clean flow outlet), which are also shown in radial distributions.

The pressure drop between the inlet and the clean air outlet is integrated and compared with the experimental data in Table 3.

Table 3. Swirl Tube Pressure Drop Comparison.

Turbulence Model	Pressure Drop (Pa)	Discrepancy (%)
RANS k- ω SST	99	52.3
RSM	84	29.2
DES	83	27.7
Experiment	65	--

It is observed that the discrepancy between the numerical analyses and experimental data is at least 27.7 %. However, RSM and DES pressure drop predictions are far close to the experimental results when compared with the k- ω SST model.

CONCLUSION

The performance of different turbulence models on predicting the high swirling flow characteristics inside cyclones are investigated. Because of the anisotropic stress characteristics of the high swirling flows, there are considerable differences between k- ω SST turbulence model results and the experiments as expected. Beside the discrepancies in magnitudes, it is observed that, the flow characteristics are also wrong especially on the regions close to the centerline. Resulting pressure drop discrepancies can also exceed 50 % with this turbulence model.

On the other hand, it is observed that the RSM analyses are in fairly good agreement with test data particularly in Stairmand cyclone case. Although, the swirl tube cyclone results are not predicted as well as Stairmand cyclone, they are aligned with the literature, [Hoekstra, 2000]. The velocity distribution appears to be similar to solid body rotation in the experiments and this behavior is captured in RSM solutions. The pressure drop differences are also reduced considerably with this turbulence model. As a result of the relatively high discrepancies in the swirl tube case, a hybrid turbulence model, namely the Detached Eddy Simulation (DES), is also tested on this case.

It is important to note that, DES and other hybrid methods are computationally much more expansive than RANS and RSM models. This additional effort mostly comes from the necessity of conducting unsteady analysis on DES method. For the specific cases shown in this study, DES analysis approximately takes thirty times of the computation time needed for the RANS solutions, Figure 9 shows that DES model predicts centerline velocity magnitude and the increase slope very well, but the differences increase with radial distance. The improvement on integral parameters such as pressure drop cannot justify the extra computational effort needed.

References

- Barth, W. (1956) *Berechnung und Auslegung von Zyklonabscheidern auf Grund Neuerer Untersuchungen*, Brennst. Warme Kraft. 8. pp 1-9.
- Leith, D. and Licht, W. (1972) *Collection Efficiency of Cyclone Type Particle Collectors – a New Theoretical approach*, Am. Inst. Chem. Engng. Symp. Ser. Air-1971. 68, pp 196-206.
- Ioia, D.L. and Leith, D. (1989) *Effect of Cyclone Dimensions on Gas Flow Pattern and Collection Efficiency*, Aerosol Sci. Technol. 10, pp 491-500.
- Griffiths, W.D. Boysan, F. (1996) *Computational Fluid Dynamics (CFD) and Empirical Modelling of the Performance of a Number of Cyclone Samplers*, J. Aerosol Sci., 98, pp 281-304.
- Sylvia, N. Yunardi, Maulana, I. Elwina, Wusnah, Bindar, Y. (2011) *Analysis of Turbulence Models Performance for the Predictions of Flow Yield, Efficiency and Pressure Drop of Gas-Solid Cyclone Separator*, Proc. Of the Annual Conference Syiah Kuala University, November 29-30.
- Gimbun, J. Choong, T.S.Y. Chuah, T.G. Fakhru'l-Razi, A. (2005) *A CFD Study on the Prediction of Cyclone Collection Efficiency*, Int. J. for Comp. Methods in Engineering Sci. and Mech., 6(3), pp161-168.
- Wang, B., Xu, D.L., Xiao, G. X., dan Yu, A.B. (2005) *Numerical Study of Gas-Solid Flow in a Siklon*, Appl Math Model, 30:1326-1342.
- Hoekstra, A.J. Derksen, J.J. Van Der Akker, H.E.A. (1999) *An Experimental and Numerical Study of Turbulent Swirling Flow in Gas Cyclones*, Chemical Engineering Science 54, 2055-2065.
- Hoekstra, A.J. (2000) *Gas Flow Field and Collection Efficiency Cyclone Separators*, PhD Thesis, Technical University of Delft.